Arteriosclerosis, Thrombosis, and Vascular Biology

TRANSLATIONAL SCIENCES

Vitamin D Receptor From VSMCs Regulates Vascular Calcification During CKD: A Potential Role for miR-145a

Maite Caus, Cristina Alonso-Montes, Jose Luis Fernandez-Martin, Manuel Marti-Antonio, Milica Bozic,* Jose M. Valdivielso*

BACKGROUND: Vascular calcification (VC) is a highly prevalent complication of chronic kidney disease (CKD) and is associated with the higher morbidity-mortality of patients with CKD. VDR (vitamin D receptor) has been proposed to play a role in the osteoblastic differentiation of vascular smooth muscle cells (VSMCs), but the involvement of vitamin D in VC associated to CKD is controversial. Our aim was to determine the role of local vitamin D signaling in VSMCs during CKD-induced VC.

METHODS: We used epigastric arteries from CKD-affected patients and individuals with normal renal function, alongside an experimental model of CKD-induced VC in mice with conditional deletion of VDR in VSMC. In vitro, experiments in VSMC with or without VDR incubated in calcification media were also used.

RESULTS: CKD-affected patients and mice with CKD showed an increase in VC, together with increased arterial expression of VDR compared with controls with normal renal function. Conditional gene silencing of VDR in VSMCs led to a significant decrease of VC in the mouse model of CKD, despite similar levels of renal impairment and serum calcium and phosphate levels. This was accompanied by lower arterial expression of OPN (osteopontin) and lamin A and higher expression of SOST (sclerostin). Furthermore, CKD-affected mice showed a reduction of miR-145a expression in calcified arteries, which was significantly recovered in animals with deletion of VDR in VSMC. In vitro, the absence of VDR prevented VC, inhibited the increase of OPN, and reestablished the expression of miR-145a. Forced expression of miR-145a in vitro in VDR^{wt} VSMCs blunted VC and decreased OPN levels.

CONCLUSIONS: Our study provides evidence proving that inhibition of local VDR signaling in VSMCs could prevent VC in CKD and indicates a possible role for miR-145a in this process.

GRAPHIC ABSTRACT: A graphic abstract is available for this article.

Key Words: microRNAs ■ osteopontin ■ receptors, calcitriol ■ renal insufficiency, chronic ■ vascular calcification

Vascular calcification (VC) is characterized by the abnormal deposition of calcium (Ca) phosphate salts in the tunica media of blood vessels. VC is highly prevalent in patients with chronic kidney disease (CKD),[1,2] and it is a strong predictor of cardiovascular mortality in CKD population.[3–5] The major form of VC in CKD is medial VC, where vascular smooth muscle cells (VSMCs) play an essential role. VSMCs are the predominant cells of the vascular wall with a contractile phenotype and an important role in maintaining vessel function. During VC, VSMCs undergo a nonreversible phenotypic transformation consisting in the loss of their smooth muscle phenotypic markers, acquisition of the osteogenic phenotype with upregulation of bone-specific genes such as *Runx2* (runt-related transcription factor 2), *BMP-2*, *alkaline phosphatase*, *OPN* (osteopontin), *osteocalcin*, and *lamin A*[6–10] and downregulation of VC inhibitors such as SOST (sclerostin), fetuin-A, and MGP (matrix Gla protein).[7,8,11,12]

Correspondence to: Milica Bozic, PhD, Vascular and Renal Translational Research Group, Institute for Biomedical Research in Lleida, Edificio Biomedicina 1, Lab B1-10, Rovira Roure 80, 25198 Lleida, Spain, Email milica.bozic@irblleida.udl.cat; or Jose M. Valdivielso, PhD, Vascular and Renal Translational Research Group, Institute for Biomedical Research in Lleida, Edificio Biomedicina 1, Lab B1-10, Rovira Roure 80, 25198 Lleida, Spain, Email josemanuel.valdivielso@udl.cat
*M. Bozic and J.M. Valdivielso share senior authorship.
Supplemental Material is available at https://www.ahajournals.org/doi/suppl/10.1161/ATVBAHA.122.318834.
For Sources of Funding and Disclosures, see page 1547.

Arterioscler Thromb Vasc Biol is available at www.ahajournals.org/journal/atvb

Nonstandard Abbreviations and Acronyms

1,25D	1α-25-dihydroxyvitamin D_3
Ca	calcium
CKD	chronic kidney disease
CM	calcification medium
MGP	matrix Gla protein
miRNA	microRNA
NM	normal medium
OPN	osteopontin
P	phosphorus
PCR	polymerase chain reaction
RT	room temperature
SOST	sclerostin
Tx	tamoxifen
VC	vascular calcification
VDR	vitamin D receptor
VSMC	vascular smooth muscle cell
WT	wild type

Highlights

- VDR (vitamin D receptor) is one of the main characters for vascular calcification progression.
- OPN (osteopontin) mediates calcification regulated by VDR.
- miR-145a is involved in calcification and protects against it.
- VDR inhibition protects from vascular calcification.

Despite many studies being undertaken, the molecular mechanisms implicated in VC are not entirely understood.

Vitamin D is a steroid hormone that acts as a transcription factor by binding to its receptor (VDR [vitamin D receptor]), with the ability to regulate different osteogenic genes through vitamin D response elements[13,14] in the promoter regions of target genes. It has been demonstrated that VSMCs have functional VDR[15] and that the active vitamin D compound 1α-25-dihydroxyvitamin D_3 (1,25D) directly increases VSMC calcification in vitro.[13] In the last 2 decades, active vitamin D compounds have been used in patients with CKD to control secondary hyperparathyroidism, but the effect of vitamin D on VC is not entirely clear.[16] Thus, Shroff et al[17] demonstrated that either high or low levels of vitamin D are associated with increased VC[18] in pediatric patients, while Lomashvili et al[19] pointed to a systemic action rather than a direct vascular effect of vitamin D on an experimental model of VC. Interestingly, Han et al[20] reported that VDR deficiency protected against VC, as aortas from total VDR^{ko} mice presented complete inhibition of VC induced by high vitamin D. Although the existence of physiologically active VDR and its actions in VSMCs have been widely described,[21] details on the role of local VDR signaling in VC are still lacking.

Accumulating evidence points to microRNAs (miRNAs) as important players in the process of VC. A diversity of miRNAs has been demonstrated to promote VC, while others seem to have a protective role.[22,23] miRNAs are small endogenous, noncoding, single-stranded RNA molecules able to regulate gene expression through posttranscriptional processing of mRNAs.[24] Recent studies show that miR-145 expression decreases in transdifferentiated VSMCs of rats with CKD,[25] as well as in human cultured VSMCs exposed to high levels of phosphate.[26] In addition, VDR has been considered as a potent regulator of these small molecules, and miR-145 was identified as a target for 1,25D.[27]

In the present study, we combine experimental studies using VSMC cultures in vitro and conditional knockout mice with the specific deletion of VDR in VSMCs, with human samples of patients with CKD to study the role of local VDR signaling in medial VC during CKD.

MATERIALS AND METHODS

Data Availability

The data that support the findings of this study are available from the corresponding author upon reasonable request and in the Supplemental Material.

Human Epigastric Artery Samples

Human arterial samples were obtained from consecutive CKD patients who underwent a renal transplantation procedure in Hospital Universitario Central de Asturias between 2011 and 2012 (n=15) and from healthy kidney donors (n=17) with normal renal function, nonsmokers, and free from diabetes and cardiovascular disease. Studies involving human samples were performed in agreement with the Declaration of Helsinki and with local and national laws. The Human Ethics Committee of the Hospital Universitario Central de Asturias approved the study procedures (CEImPA: 2022.240). All participants signed an informed consent before inclusion in the study providing permission for their medical data to be anonymously used for the research.

Animal Study

All animal studies were approved by the local Ethics Committee of the University of Lleida (2014-0046) and complied with all relevant ethical regulations and guidelines of the European Research Council for the Care and Use of Laboratory Animals.

Mice were housed and maintained in a barrier facility, and pathogen-free procedures were used in all mouse rooms. Animals were kept in a 12-hour light/dark cycle at 22 °C with ad libitum access to food and water. Animals were weaned at 21 days. After weaning, they were maintained on a regular mouse chow (Harlan Teklad, Madison, WI).

VDR^{ko} mice on a B6CBA genetic background were backcrossed for >8× to C57BL/6J mice and have been maintained

in our colony for >12 years. VDR^{ko} mice were fed a high-Ca, high-phosphate diet (rescue diet; TD-96348, 20% lactose, 2% Ca, 1,25% phosphorus [P]; Harlan Teklad) to prevent hypocalcemia. Two-month-old VDR^{wt} and VDR^{ko} male mice were used for all in vitro experiments. Mice were genotyped by tail biopsy polymerase chain reaction (PCR) using VDR^{wt}- and VDR^{ko}-specific primers as described previously[28] (genotyping details are available in the Supplemental Material).

Generation of the Conditional VSMC-Specific VDR Null Mice

To generate conditional VSMC-specific VDR null mice, VDR^{lox} mice on a Swis 129 background (kindly provided by Dr Geert Carmeliet from the Leuven University)[29] were bred with Myh11 (myosin heavy chain 11)-CreER^{T2} transgenic mice (Cre recombinase under the control of the smooth muscle myosin heavy chain promoter) on a C57BL/6J background (kindly provided by Dr Juan Miguel Redondo Moya from CNIC (Centro Nacional de Investigaciones Cardiovasculares) after being generated by Dr Stefan Offermanns)[30] to yield Myh11-CreER^{T2}+ VDR$^{wt/lox}$ progeny. Myh11-CreER^{T2}+ VDR$^{wt/lox}$ mice were intercrossed to obtain the breeders that will produce experimental genotypes Myh11-CreER^{T2}+ VDR$^{wt/wt}$ (control group) and Myh11-CreER^{T2}+ VDR$^{lox/lox}$ (arterial VSMC-specific deletion of VDR; further called Cre+ VDR$^{wt/wt}$ and Cre+ VDR$^{lox/lox}$). Mice were genotyped by tail biopsy PCR using Cre transgene and VDR^{loxP}-specific primers, as explained in the Supplemental Material. VDR was deleted from the arterial VSMCs using the CRE-loxP recombination system induced by tamoxifen (Tx). Eight-week-old male Cre+ VDR$^{wt/wt}$ and Cre+ VDR$^{lox/lox}$ mice were injected with Tx dissolved in corn oil (1.5 mg/day during 5 days). Male mice of each genotype without Tx injection served as corresponding controls. Only males could be used for the experiment because the Myh11-CreER^{T2} BAC transgene was inserted in the Y chromosome.

To assess the specificity of Cre recombinase expression, Myh11-CreER^{T2} mice were crossed with reporter mT/mG (B6.129[Cg]-Gt[ROSA]26Sor$^{tm4(ACTB-tdTomato-EGFP)Luo/J}$) mice, obtained from The Jackson Laboratory (Bar Harbor, ME). The mT/mG ROSA reporter mice express red fluorescence before and green fluorescence following Cre-mediated recombination.

Mouse Model of VC in CKD

Subtotal nephrectomy was performed under general anesthesia in 8-week-old Cre+ VDR$^{wt/wt}$ and Cre+ VDR$^{lox/lox}$ male mice, as described previously.[31] Briefly, 1 week after Tx injection, mice were subjected to 2-step surgical procedure for 75% nephron reduction. In the first step, the parenchyma of the left kidney was reduced by 50%. The kidney was exposed, decapsulated, and carefully cauterized, reducing the parenchyma of the upper and the lower pole. In the sham-operated mice of both genotypes, left flank incision was performed, kidney was manipulated, and the flank incision was closed. One week after the recovery, right-sided total nephrectomy was performed and a second simulated operation was performed in the sham group. Isoflurane was used as an anesthetic during the surgery, and buprenorphine (0.05 mg/kg, sc) was used as an analgesic following both surgeries. One week after the right-sided total nephrectomy, mice were switched to a high-phosphate diet (0.9% P and 0.6% Ca, C1031; Altromin) and treatments with 1,25D (500 ng/kg; Kern Pharma) 3× per week during 2 months started. At the end of the experiment, 24-hour urine was collected and mice were euthanized by cardiac exsanguination. Blood was collected by cardiac puncture, and animals were then perfused with ice-cold PBS through a puncture in the left ventricle. Aorta and kidney samples were collected for histologic examination and molecular analysis. One part of the artery and kidney was fixed in 4% paraformaldehyde/PBS for histologic examinations after embedding in paraffin or Bright Cryo-M-Bed compound (Bright Instrument Co). The remaining aortic and kidney tissue was snap-frozen in liquid nitrogen and kept at −80 °C for protein and mRNA extractions.

Serum and Urine Biochemical Analysis

Serum P and Ca were determined by standard clinical methods using a multichannel Hitachi Modular analyzer (Roche Diagnostics, Indianapolis, IN) of the Biochemistry service of the University Hospital Arnau de Vilanova. Inorganic phosphate was determined by the ammonium molybdate method and Ca with the o-cresolphtalein complexone method. Blood urea nitrogen was determined by colorimetric assay using the Urea 37 kit (Spinreact, Girona, Spain).

Histologic Examination and Immunohistochemistry

Immunostaining for VDR (sc-1008; Santa Cruz Biotechnology, Inc, CA), Runx2 (NBP1-01004; Novus Biological, Littleton, CO), SOST (No. AF1589), and OPN (No. AF808) from R&D Systems was performed on 5-µm-thick tissue sections of human epigastric arteries or mouse aortas. Tissue sections were deparaffinised through xylene and rehydrated through graded ethanol concentrations into distilled water, as described previously.[32] Briefly, antigen retrieval was done by boiling the slides in 10 mM citrate buffer (pH 6) for 15 minutes. Endogenous peroxidase quenching (30-minute incubation in 0.66% [vol/vol] H_2O_2/PBS) was followed by blocking of nonspecific binding with 3% BSA/PBS (for VDR immunostaining) or horse serum (PK-6200; Vector Laboratories, Burlingame, CA) for other proteins, 30 minutes at room temperature (RT). Primary anti-VDR (1/100), anti-Runx2 (1/50), anti-SOST (1/50), and anti-OPN (1/50) were incubated overnight at 4 °C. After washing with PBS, slides were treated with corresponding biotinylated secondary antibody (30 minutes, RT), which was followed by the avidin-biotin-peroxidase complex (30 minutes, RT) and 3,3′-diaminobenzidine as a chromogen (10 minutes, RT; Vector Laboratories). Sections were counterstained with Mayer hematoxylin to visualize the nuclei. Negative controls were performed by incubation with nonimmune serum or 3% BSA/PBS instead of the specific primary antibody, which resulted in a complete absence of staining. Finally, samples were dehydrated and mounted with DPX medium. Stained tissue sections were examined using an Olympus BX50 microscope with an Olympus automatic camera system. Immunohistochemical results of VDR staining were evaluated following the uniform preestablished criteria. Staining intensity and percentage of positive cells were graded semiquantitatively. Histological scores were obtained from each sample as follows: histoscore=1×(%light staining)+2×(%moderate staining)+3×(%strong staining), which ranged from 0 (no immunoreaction) to 300 (maximum immunoreactivity). The reliability of such scores for interpretation of immunohistochemical staining of tissue sections has already been demonstrated previously.[33]

Ca deposits in mouse aortic paraffin sections (5 µm) were stained using Alizarin red. Samples were deparaffinized, rehydrated, and stained in 50 mM Alizarin red solution at pH between 4.1 and 4.3 for 5 minutes at RT. After staining,

samples were dehydrated with acetone, acetone-xylene (1:1), and mounted in synthetic mounting medium (DPX, Vitro-Clud). Ca deposits from human epigastric arteries were visualized by Von Kossa staining as described previously.[34] Briefly, deparaffinized, hydrated artery sections were incubated in 5% silver nitrate before the revealing solution. Slides placed in 2% sodium thiosulfate were counterstained with nuclear fast red.

Arteries and kidneys from reporter mice embedded in Bright Cryo-M-Bed compound were cut in 8-µm-thick tissue sections and were used to determine mT/mG expression switch. Fluorescence was analyzed using an Olympus FluoView FV1000 confocal laser-scanning microscope with a digital camera system.

Aortic Ca Quantification

Aortic tissue was homogenized in hydrochloric acid 1 N, using TissueLyser LT (8 cycles of 1 minute), and incubated in the same solution on vortex shaker to enable decalcification for 16 hours at 4 °C. After centrifugation, the supernatant was collected and Ca content was determined colorimetrically using the cresolphtalein complexone method. Protein content from the pellet was determined by DC protein assay kit (Bio-Rad, Hercules, CA). Aortic Ca content was normalized to protein amount and expressed as micrograms of Ca per milligrams of protein.

In Vitro Study

Primary Mouse VSMC Cultures and Induction of Calcification

Primary mouse aortic smooth muscle cells (VSMCs) from 8-week-old male VDR^{wt} and VDR^{ko} mice were obtained by explant culture as described previously.[35,36] VSMCs were maintained in DMEM (41966-029; Gibco, ThermoFisher Scientific, Waltham, MA) containing 20% of fetal bovine serum, 100 U/mL penicillin, and 100 µg/mL streptomycin. The media was replaced every 2 to 3 days. For calcification experiments, cells were seeded in 6-well plates (70 000 cells per well) and treated during 6 days with calcification medium (CM) composed of DMEM (41966-029), sodium pyruvate (10 mM), 10 mM β-glycerophosphate (Sigma-Aldrich), and 5% of normal rat serum, with a final concentration of Ca adjusted to 6 mM. Control cells were treated with normal medium (NM) composed of DMEM (41966-029; Gibco) containing 5% fetal bovine serum. Fresh treatment media with supplements was replaced every 3 days. At the sixth day of the treatment, cells were serum deprived overnight and subsequently harvested for RNA extraction or Ca determination. VSMCs between passages 2 and 6 were used in all experiments.

Determination of VSMC Calcification In Vitro

At the end of the experiments, total Ca content was quantified using the o-cresolphtalein complexone method as reported previously.[37] Briefly, cells were collected with PBS and centrifuged. Pellet was resuspended with 25 µL of hydrochloric acid 0.6 N and mixed by vortexing at 4 °C overnight. After centrifugation, supernatant was collected for Ca quantification and the remaining pellet was used to quantify protein content.

For the Alizarin red staining, VSMCs incubated in NM or CM were washed with PBS 2× and then fixed with 10% formaldehyde at RT for 15 minutes. After fixation, cells were washed with H_2O and incubated with 40 mM Alizarin red solution (Sigma A3757; Sigma-Aldrich, St. Louis, MO), pH 4.1 to 4.3, for 20 minutes at RT. Alizarin red staining was examined using an Olympus BX50 microscope with an Olympus automatic camera system.

Primary Human VSMC Culture

Human aortic VSMCs (CRL-1999; ATCC [American Type Culture Collection], Manassas, VA) were cultured in DMEM containing 20% fetal bovine serum, 100 U/mL penicillin, and 100 µg/mL streptomycin. Cells were used between passages 3 and 8, incubated in 37 °C humid atmosphere with 5% CO_2. Medium was replaced every 2 to 3 days. For experiments, cells were seeded in 6-well plates (75 000 cells per well) and treated during 6 days with 1,25D (D1530-10UG; Sigma-Aldrich).

Vitamin D Incubation

Human and mouse VSMCs were treated with 1,25D, which was dissolved in 95% ethanol and added to the culture medium to a final concentration of 1, 10, or 100 nM for 6 days. Fresh medium with 1,25D was replaced at day 3 of the experiment.

Transfection of VSMCs With miR-145a Mimic or miR-145a Inhibitor

Mouse VDR^{wt} VSMCs were transfected with mmu-miR-145a-5p mimic (mirVana mRNA mimic; Applied Biosystems), mmu-miR-145a-5p inhibitor (mirVana miRNA inhibitor; Applied Biosystems), or the corresponding mirVana miRNA negative control, at final concentration of 50 nM each, using Lipofectamine RNAiMAX (Invitrogen) and following manufacturer's instructions. After 24 hours, transfection medium was replaced with fresh medium (NM or CM, depending on the experiment). At the third day of the treatment, cells were retransfected with miR-145a-5p mimic, miR-145a-5p inhibitor, or negative control. VSMCs were kept in NM or CM for the following 3 days.

Quantitative Real-Time PCR

Total RNA was extracted from aorta using RNA isolation kit (Macherey-Nagel) and from cultured cells using TRIzol reagent (Molecular Research Center, Inc), following manufacturer's instructions. Reverse transcription was performed with First Strand cDNA Synthesis Kit (Applied Biosystems) according to manufacturer's instructions. Real-time PCR with gene-specific TaqMan probes for mouse *VDR* (Mm.PT.58.8581722), *lamin A* (Mm.PT.58.12742897; Integrated DNA Tech, Inc, Madrid, Spain), *OPN* (Mm00436767_m1), *Runx2* (Mm00501584_m1), *SOST* (Mm04208528_m1), and *TBP* (TATA box binding protein; Mm00446971_m1; Applied Biosystems) was performed with a QuantStudio 7 Real-Time PCR detection system (Applied Biosystems), using TaqMan Universal PCR Master Mix, No AmpErase UNG. Forty cycles at 95 °C for 17 s and 60 °C for 1 minute were performed. Duplicate readings were taken, and the average was calculated.

miR-145a (002278), miR-155 (002571), miR-30c (000419), miR-146a (000468), miR-29b (000413), and U6 (001973) reverse transcription was performed using TaqMan miRNA Reverse Transcription Kit (Applied Biosystems) according to the manufacturer's protocol. The expression of different miRNAs and U6 were measured using TaqMan miRNA assays and TaqMan Universal PCR Master Mix II no AmpErase UNG (Applied Biosystems).

Relative mRNA and miRNA levels were calculated by standard formulae (ΔΔCt method) using TBP or U6 as endogenous controls, respectively. The results referred to a randomly selected basal sample considered as value 1.0.

Western Blot Analysis

Aortic tissue was homogenized in NP-40 buffer (20 mM Tris [pH 7.4], 140 mM NaCl, 10% glycerol, 1% Ca-630, 2 mM PMSF [phenylmethylsulfonyl fluoride], 1 mM Na_3VO_4, and protease inhibitor cocktail) using the TissueLyser LT (Qiagen, Hilden, Germany). Four cycles of homogenization were performed (50 Hz, 1 minute for each cycle), followed by 3 cycles in liquid nitrogen and thawing at 37 °C. The supernatant was collected and centrifuged for 10 minutes at 1100*g*, at 4 °C.

Total cell lysates were obtained by washing the cell monolayer with cold PBS, scraping and suspending in SDS buffer (50 mM Tris–hydrochloric acid, pH 7.5; 150 mM NaCl; 1% Triton X-100; 2% SDS; 1% Na-deoxycholate; 1% Igepal; and 0.5 μM EDTA).

Protein concentrations were determined using a DC protein assay kit (Bio-Rad, Manassas, VA). The samples were electrophoresed on 8% or 10% SDS-PAGE gels and transferred to PVDF (polyvinylidene difluoride) membranes (Immobilon-P; Milipore, Billerica, MA). Membranes were blocked for 1 hour with 5% skim milk in Tris-buffer saline solution containing 0.1% Tween-20 and subsequently probed with primary antibodies against VDR (1:000; Santa Cruz, CA), OPN (1:1000; R&D Systems, Bio-Techne), Runx2 (1:1000; Novus Biological), and GAPDH (1:10 000; Abcam), overnight, at 4 °C. Horseradish peroxidase-conjugated secondary antibodies (anti-rabbit [Cell Signaling], anti-goat [Santa Cruz], or anti-mouse [Jackson Immunoresearch]) were used at 1/10 000 for 1 hour at RT. The immunoreaction was visualized using chemiluminescent kits EZ ECL (Biological Industries, Kibbutz Beit Haemek, Israel) or ECL Advanced (Amersham Biosciences, Little Chalfont, United Kingdom). Images were digitally acquired by ChemiDoc MP Imaging system (Bio-Rad). Positive immunoreactivity bands were quantified by densitometry and compared with the expression of adequate loading control.

Statistical Analysis

Statistical analysis was performed using SPSS V27 (IBM Corp, Armonk, NY) and R Statistical Software (v4.1.2; R Core Team 2021) with the package bestNormalize. All data examined are expressed as mean±SEM. The normality of the distributions was assessed by the Shapiro-Wilk test and the homogeneity of variance by the Levene test. Transformation of the data was performed when needed to achieve normality and homoscedasticity. Untransformed data are presented in the graphs. Comparisons between 2 groups was performed by Student *t* test with or without Welch correction, depending on the homogeneity of variances and by Mann-Whitney *U* test for non-normal distributions presenting homoscedasticity. Comparisons between >2 homoscedastic groups were performed by 1-way ANOVA or with the Kruskal-Wallis test, depending upon normality of the distribution, with a post hoc pairwise comparison with the Bonferroni test. When 2 groups and 2 treatments were tested, a 2-way ANOVA was used with a post hoc pairwise comparison with the Tukey HSD test. $P<0.05$ was considered statistically significant.

RESULTS

VDR Expression Is Induced in Calcified Arteries of Patients and Mice Affected by CKD

To investigate the potential role of VDR in VC during CKD, we analyzed epigastric arteries from patients with CKD subjected to kidney transplantation and non-CKD donors (see patients' characteristics in Table S1). Arteries from patients with CKD showed a significant increase in Ca levels compared with non-CKD donors (Figure 1A). Results were corroborated by arterial Von Kossa staining (Figure 1C). Of note, immunostaining for VDR was also significantly higher in calcified arteries of patients with CKD than in arteries obtained from control non-CKD donors (Figure 1B and 1C), which was confirmed by Western blot results (Figure S1).

Next, we assessed the expression of arterial VDR in our experimental mouse model of VC in CKD. Mice subjected to 5/6 nephrectomy, a widely used model of CKD, showed higher levels of Ca content in their arteries compared with control mice (Figure 2A). CKD significantly increased the expression of VDR mRNA (Figure 2B) and protein levels in arteries from CKD animals (Figure 2C through 2F).

Altogether, our results demonstrate that arterial VDR is induced in mouse model of VC in CKD, as well as in patients affected by CKD who also show increased VC.

VSMC-Specific VDR Gene Deletion in Mice

To assess the role of VSMC's VDR in the development of VC during CKD, we generated mice with a specific deletion of VDR in VSMCs by crossing homozygous VDR^{lox} mice with Myh11-$CreER^{T2}$ transgenic mice. PCR analysis of tail DNA confirmed the genotypes of VSMC-specific VDR null mice (Cre+ $VDR^{lox/lox}$) and the control WT (wild type) mice (Cre+ $VDR^{wt/wt}$; Figure S2A and S2B). Bands of WT or floxed VDR alleles were observed at ≈368 and 250 bp, respectively. The expression of Cre transgene (Myh11-$CreER^{T2}$) was visualized by the detection of 2 bands at 200 and 300 bp. Confirmation of the VDR exon 2 deletion from the artery was done by performing a PCR analysis of the arterial DNA, which generated a fragment of 300 bp (Figure S2C).

To confirm specific Cre recombinase activity, we crossed Myh11-$CreER^{T2}$+ mice with reporter mT/mG (B6.129[Cg]-Gt[ROSA]26$Sor^{tm4(ACTB-tdTomato-EGFP)Luo/J}$) mice. Figure S2E demonstrates arterial EGFP (enhanced green fluorescent protein) reporter immunofluorescence expression representative of Cre recombinase activity in Myh11-$CreER^{T2}$+ $mT/mG^{+/-}$ mice injected with Tx. Only arterial VSMCs switched from red to green fluorescence, indicating that Myh11-Cre was only active in VSMCs. Arteries from mice without Tx injection showed red fluorescence, indicating absence of Cre recombinase activity. No fluorescence change was detected in other organs such as the kidney (Figure S2E).

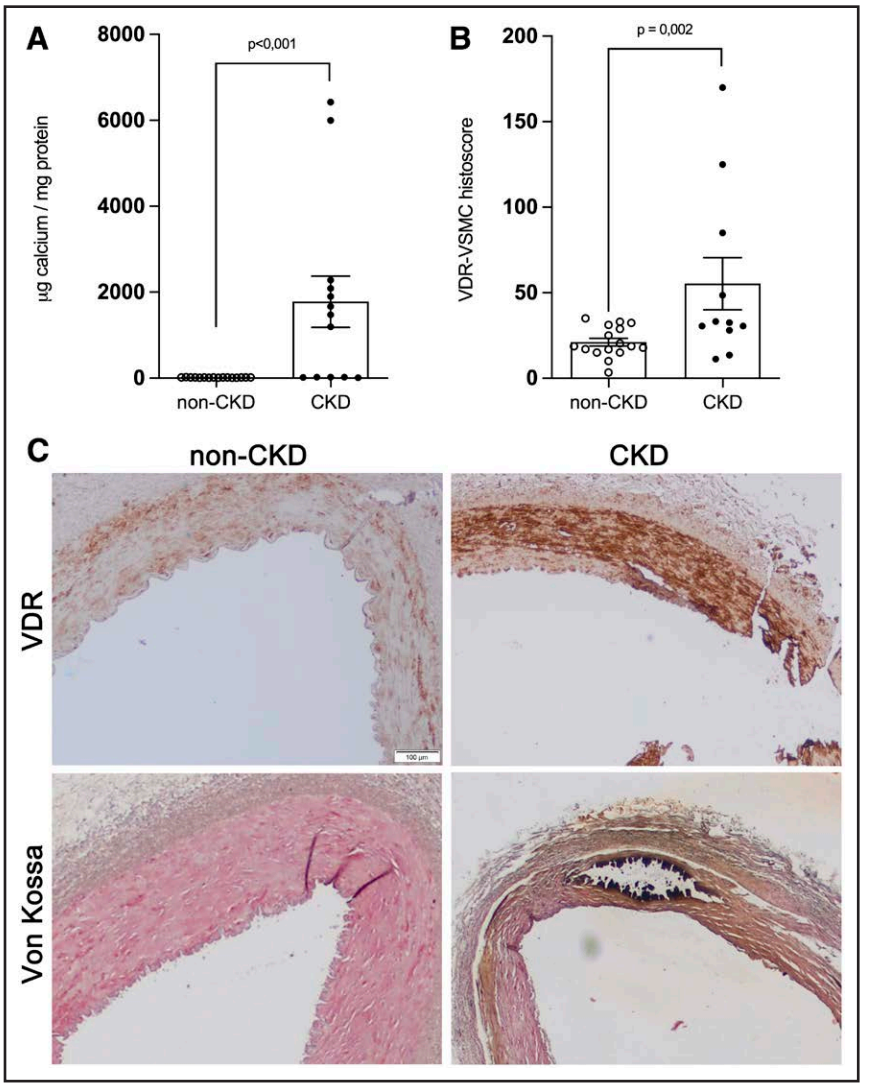

Figure 1. Increased arterial expression of VDR (vitamin D receptor) in patients with chronic kidney disease (CKD) with vascular calcification.
Vascular calcium content (**A**) and Von Kossa staining (**C**) in epigastric arteries obtained from non-CKD kidney donors and patients with CKD undergoing a renal transplant. **C**, Immunohistochemistry for VDR in arteries from patients without and with CKD. **B**, Quantification of the VDR immunostaining by histoscore. Data are presented as mean±SEM (n=16 [non-CKD] or 11–13 [CKD] patients per group). *P* values were determined by Mann-Whitney *U* test. Scale bar represents 100 µm.

Additionally, real-time PCR analysis demonstrated a significant decrease of VDR mRNA levels in aortas of Cre+ $VDR^{lox/lox}$ mice compared with Cre+ $VDR^{wt/wt}$ counterparts (Figure S2D). Immunohistochemistry and Western blot analysis confirmed qPCR results showing a marked decrease of VDR expression in Cre+ $VDR^{lox/lox}$ aortas (Figure S3A through S3C).

VDR Deletion in VSMCs Prevents VC in CKD-Affected Mice Independently of Serum Ca and Phosphate Levels

To study the effect of VSMC's VDR on VC in CKD, Cre+ $VDR^{wt/wt}$ and Cre+ $VDR^{lox/lox}$ mice were subjected to NX and treated with high-phosphate diet plus 1,25D. As expected, both Cre+ $VDR^{wt/wt}$ and Cre+ $VDR^{lox/lox}$ mice showed a marked increase of serum blood urea nitrogen (Figure 3A), suggesting a comparable degree of renal impairment. Serum Ca and P levels increased in both groups of mice affected by CKD, compared with corresponding controls (Figure 3B and 3C). Cre+ $VDR^{wt/wt}$ mice affected by CKD showed significantly higher levels of vascular Ca content (Figure 3D) and Alizarin red staining (Figure 3E through 3G) than Cre+ $VDR^{lox/lox}$ mice that underwent the same conditions (Figure 3D, 3F through 3H), indicating an evident inhibition of VC in mice with targeted deletion of VDR in VSMCs. Figure 4 shows the expression of mRNA for various markers of VC in the mouse artery. Cre+ $VDR^{wt/wt}$ mice affected by CKD showed an increased expression of OPN (Figure 4A) and lamin A (Figure 4B) mRNA in their calcified artery, which was significantly diminished in Cre+ $VDR^{lox/lox}$ counterparts. Importantly, SOST, described as a VC inhibitor, showed a marked decrease of mRNA expression in calcified arteries of Cre+ $VDR^{wt/wt}$ mice affected by CKD, while its expression recovered in Cre+ $VDR^{lox/lox}$ mice counterparts reaching almost similar levels as in the control group (Figure 4C). Runx2 mRNA increased in arteries of both Cre+ $VDR^{wt/wt}$ and Cre+ $VDR^{lox/lox}$ mice affected by CKD but without statistical difference between these 2 groups (Figure 4D). Consistent with the data from qPCR analysis, Western

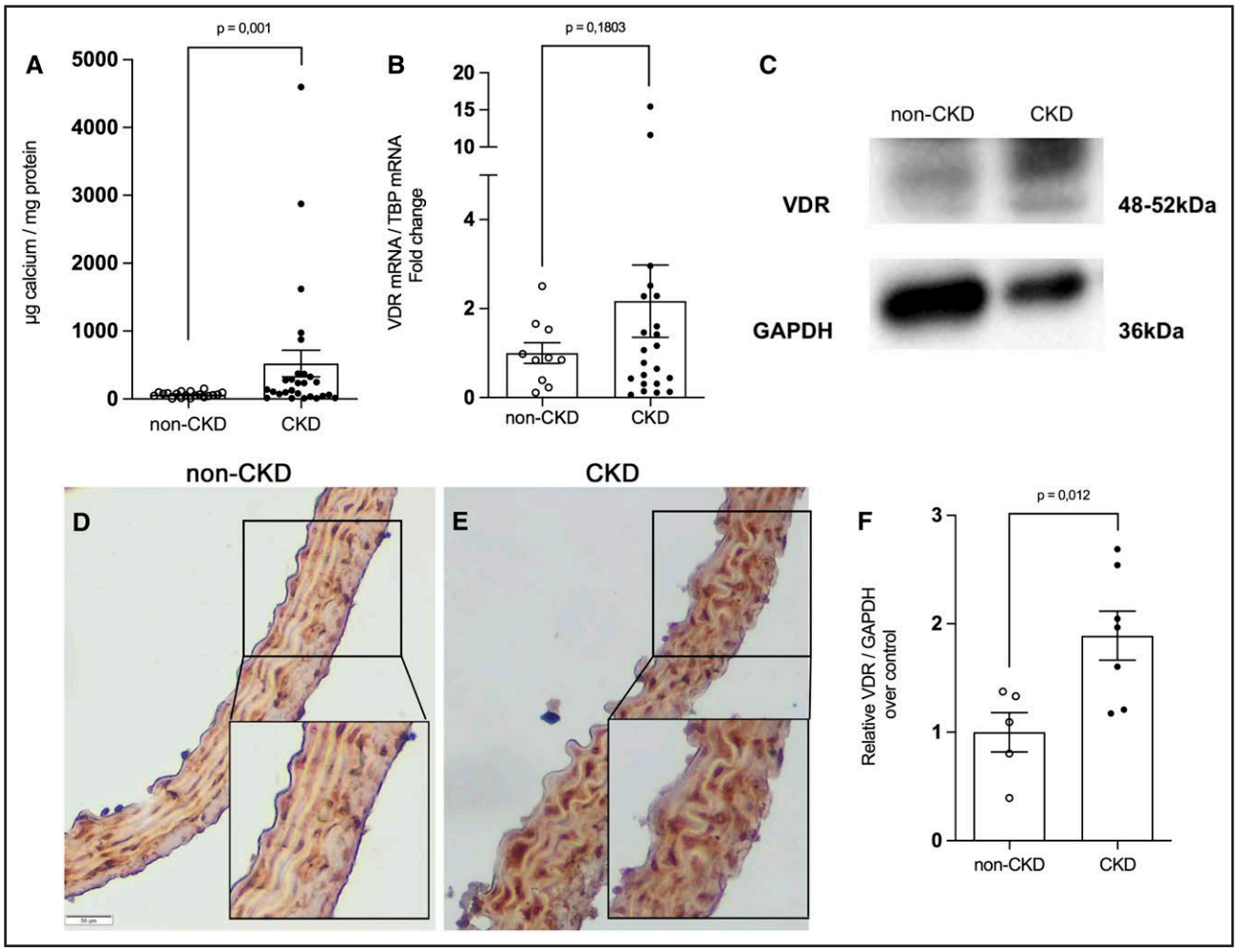

Figure 2. VDR (vitamin D receptor) increases in the experimental mouse model of vascular calcification (VC) in chronic kidney disease (CKD).

C57BL/6J mice crossed with Swis129 were used to generate a mouse model of VC in CKD, as explained in Materials and Methods. **A**, Aortic calcium content from sham-operated (non-CKD) and CKD mice was determined using an o-cresolphtalein complexone method. Data are presented as mean±SEM (n=19 [non-CKD] or 27 [CKD] mice per group). **B**, Total mRNA was extracted from arteries, and mRNA level of VDR was determined by quantitative real-time polymerase chain reaction. Relative mRNA levels were calculated and expressed as fold change over non-CKD mice (value, 1.0) after normalizing for TBP (TATA box binding protein). Data are presented as mean±SEM (n=10 [non-CKD] or 22 [CKD] mice per group). **C**, Representative Western blot analysis of VDR in arteries of both groups of mice. **F**, Quantitative analysis by densitometry. Data are presented as mean±SEM (n=5 [non-CKD] or 7 [CKD] mice per group). Representative micrographs illustrate the expression of VDR in mouse arteries of (**D**) non-CKD and (**E**) CKD mice. *P* values were determined by the Mann-Whitney *U* test or Student *t* test. Scale bar represents 50 µm.

blot showed an increased expression of OPN in calcified arteries of Cre+ $VDR^{wt/wt}$ mice affected by CKD, which was alleviated in Cre+ $VDR^{lox/lox}$ counterparts that underwent the same conditions (Figure 4F and 4H). Runx2 showed the same pattern of expression as seen in qPCR analysis, with increased levels in arteries of both CKD-affected groups of mice regardless of the arterial Ca content (Figure 4E and 4G). Immunohistochemistry corroborated Western blot and qPCR results showing higher immunoreactivity for Runx2 protein in both CKD groups. Of note, calcified arteries of Cre+ $VDR^{wt/wt}$ mice affected by CKD showed higher immunoreactivity for OPN and weaker immunostaining for SOST compared with arteries of Cre+ $VDR^{lox/lox}$ littermates (Figure 4I).

VDR Deletion From VSMCs Prevents VC of VSMCs In Vitro

To examine the effect of VDR in vitro, VSMCs were isolated from arteries of VDR^{wt} and VDR^{ko} mice, and the purity of isolated cultures was analyzed after immunofluorescence staining for αSMA (alpha smooth muscle actin), a well-known marker of VSMCs (Figure 5A). CM significantly increased Ca deposition in VDR^{wt} VSMCs compared with control cells incubated in NM (Figure 5C). Interestingly, VDR^{ko} VSMCs incubated in the CM showed significantly lower levels of Ca deposition compared with VDR^{wt} VSMCs under the same conditions (Figure 5C). The results were confirmed by Alizarin red staining (Figure 5B). Furthermore, CM led to a marked increase of OPN mRNA in VDR^{wt}

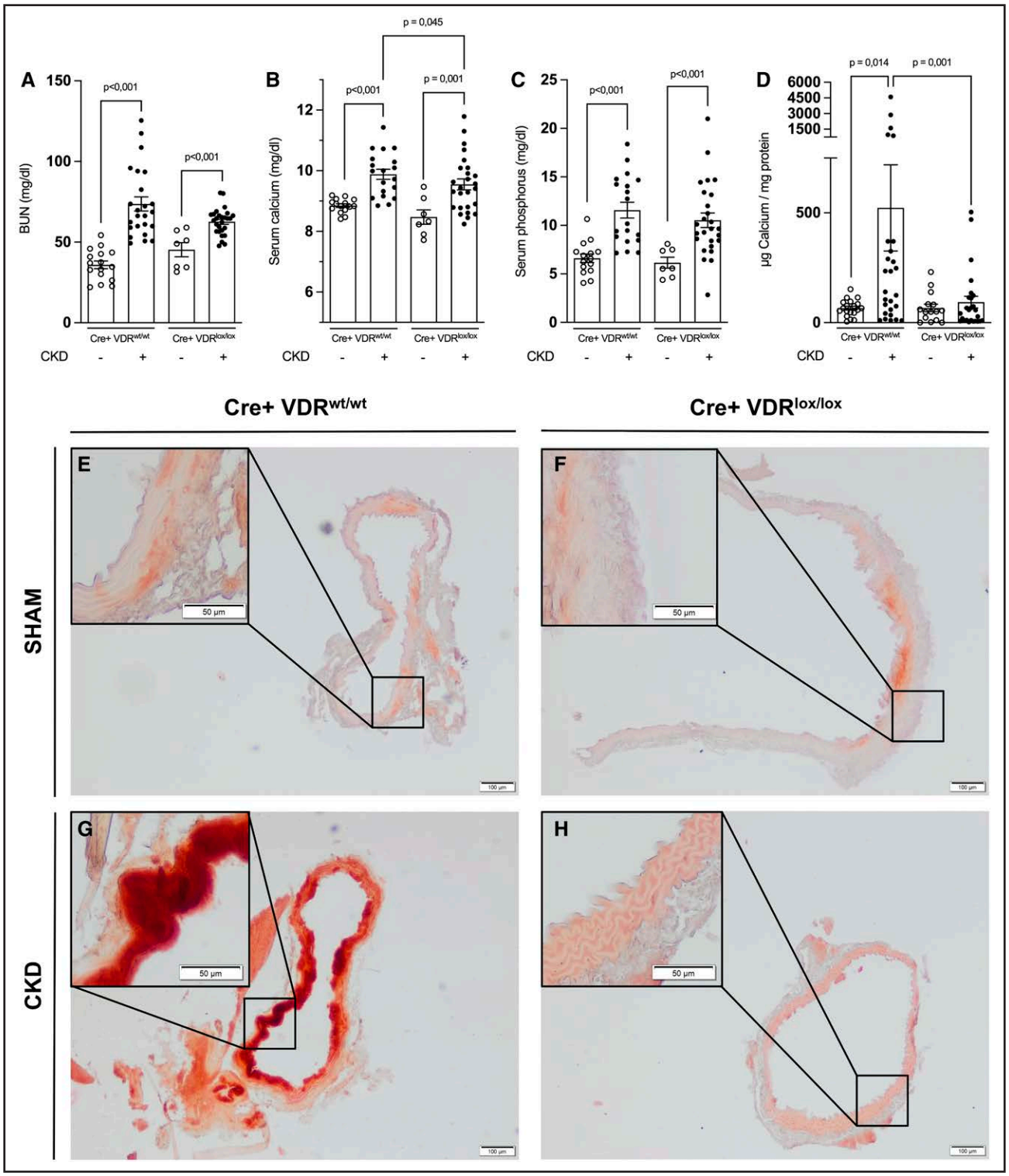

Figure 3. Deletion of VDR (vitamin D receptor) from vascular smooth muscle cells (VSMCs) of the artery prevents vascular calcification (VC) in chronic kidney disease (CKD).

Eight-week-old Cre+ $VDR^{wt/wt}$ and Cre+ $VDR^{lox/lox}$ male mice were subjected to subtotal nephrectomy and subsequently treated with high-phosphate diet (HPD) and 1α-25-dihydroxyvitamin D_3 (1,25D) for 2 months to induce VC, as explained in Materials and Methods. Serum levels of (**A**) blood urea nitrogen (BUN), (**B**) calcium, and (**C**) phosphorus. Data are presented as mean±SEM (n=7–16 [Sham control] or 19–27 [CKD] mice per group). **D**, Quantification of arterial calcium content by the o-cresolphtalein complexone method. Data are presented as mean±SEM (n=15–19 [Sham control] or 26–27 [CKD] mice per group). Representative images of Alizarin red staining of arteries from (**E**) Sham control Cre+ $VDR^{wt/wt}$, (**F**) Sham control Cre+ $VDR^{lox/lox}$, (**G**) CKD Cre+ $VDR^{wt/wt}$, and (**H**) CKD Cre+ $VDR^{lox/lox}$ mice. Scale bar represents 100 or 50 µm. *P* values were determined by post hoc pairwise comparisons after 2-way ANOVA. **A** through **D**, *P*=nonsignificant.

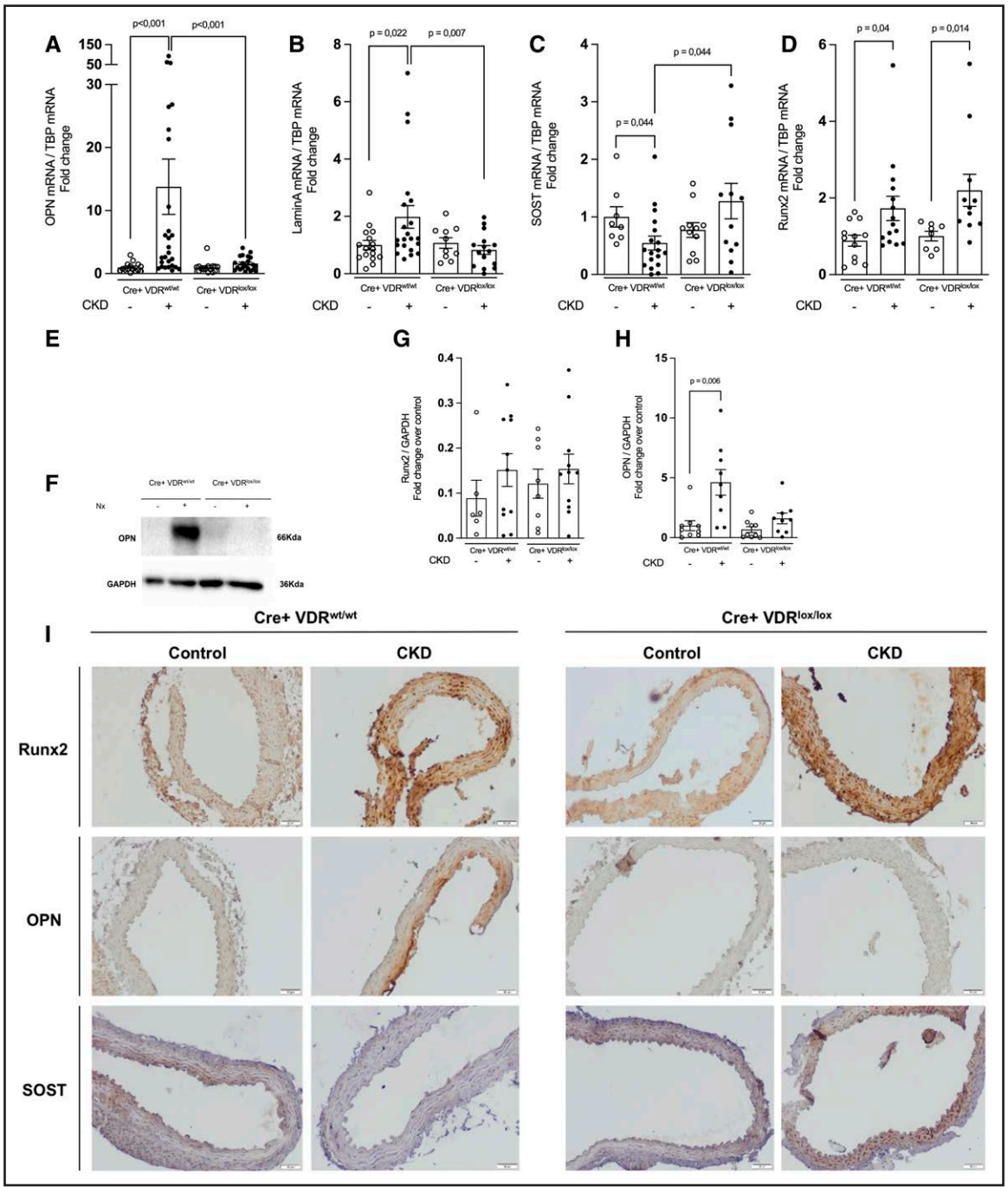

Figure 4. Deletion of VDR (vitamin D receptor) from vascular smooth muscle cells (VSMCs) of the artery modulates the expression of key osteogenic markers in a mouse model of vascular calcification (VC) in chronic kidney disease (CKD). Eight-week-old Cre+ VDR$^{wt/wt}$ and Cre+ VDR$^{lox/lox}$ male mice were subjected to subtotal nephrectomy (Nx) and subsequently treated with high-phosphate diet (HPD) and 1α-25-dihydroxyvitamin D_3 (1,25D) for 2 months to induce VC, as explained in Materials and Methods. Total mRNA was extracted from arteries, and mRNA levels of OPN (osteopontin; **A**), lamin A (**B**), SOST (sclerostin; **C**), and Runx2 (runt-related transcription factor 2; **D**) were determined by quantitative real-time polymerase chain reaction. Relative mRNA levels were calculated and expressed as fold change over Sham controls (value, 1.0) after normalizing for TBP (TATA box binding protein). Data are presented as mean±SEM (n=8–16 [Sham] or 11–27 [CKD] mice per group). **E** through **H**, Whole kidney lysates from the sham control and CKD kidneys were processed for protein analysis and were immunoblotted with antibodies against Runx2 and OPN. Representative Western blot analysis of Runx2 (**E**) and OPN (**F**) from the arteries of Cre+ VDR$^{wt/wt}$ and Cre+ VDR$^{lox/lox}$ mice subjected to Nx. **G** and **H**, Quantitative analysis by densitometry. Data were normalized to GAPDH and presented as mean±SEM (n=6–9 [Sham] or 9–11 [CKD] mice per group; fold change over sham control Cre+ VDR$^{wt/wt}$). **I**, Representative images of immunohistochemistry for Runx2, OPN, and SOST in arteries of sham control and CKD mice of both genotypes. Scale bar represents 50 µm. *P* values were determined by post hoc pairwise comparisons after 2-way ANOVA. *P*=0.034 (**A**), *P*=0.021 (**B**), *P*=nonsignificant (**C** and **D**).

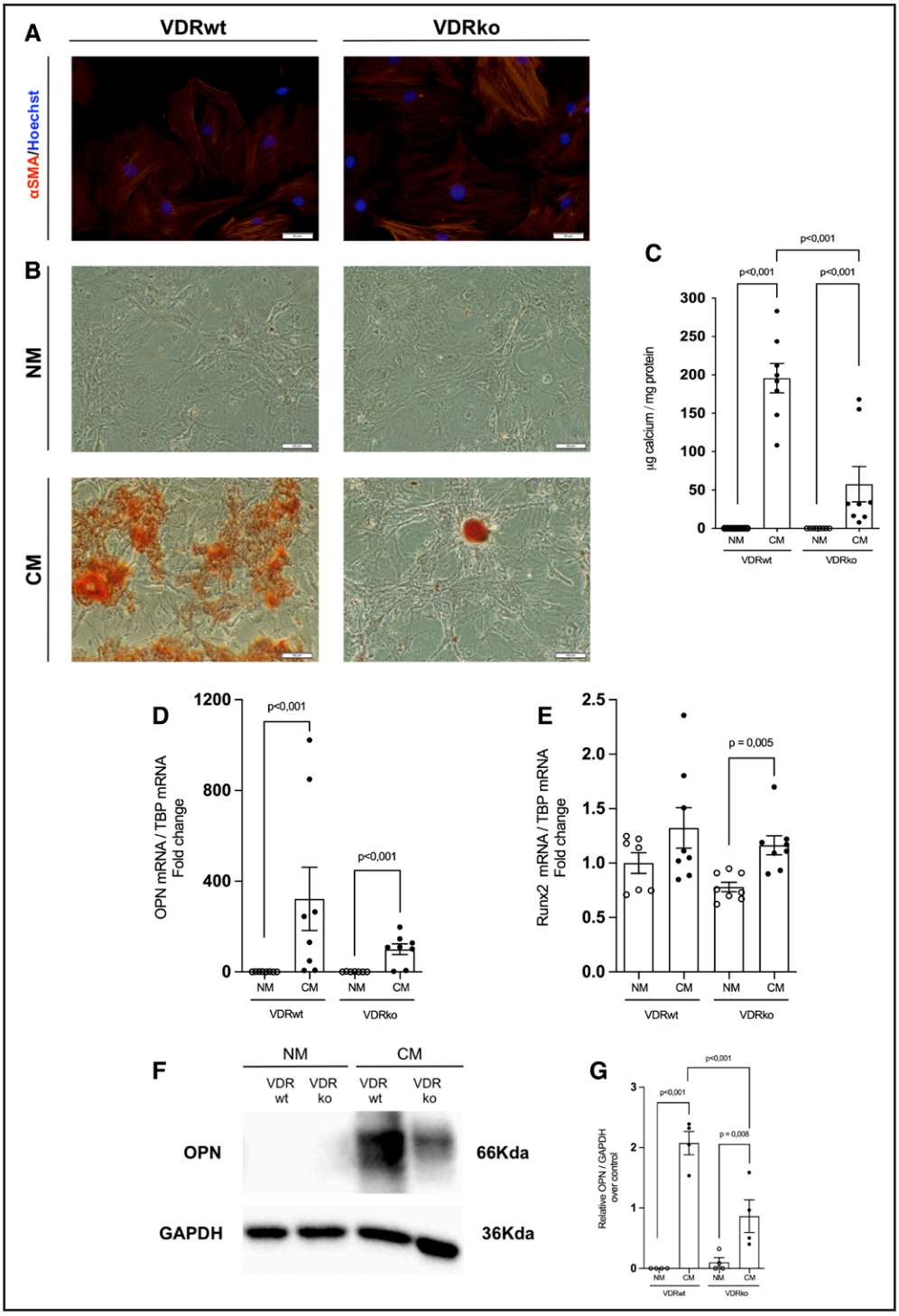

Figure 5. Depletion of VDR (vitamin D receptor) prevents calcification of vascular smooth muscle cells (VSMCs) in vitro. VSMCs were isolated from arteries of VDR^{wt} and VDR^{ko} mice and subsequently incubated in calcification (CM) or normal medium (NM) for 6 days, as explained in Materials and Methods. **A**, Immunofluorescence staining for αSMA (alpha smooth muscle actin) in VDR^{wt} and VDR^{ko} VSMCs in basal state. **B**, Alizarin red staining in VDR^{wt} and VDR^{ko} VSMC culture treated with NM or CM for 6 days. **C**, Quantification of cellular calcium content using the o-cresolphtalein complexone method. **D** and **E**, Total mRNA was extracted from VSMCs, and mRNA levels of OPN (osteopontin; **D**) and Runx2 (runt-related transcription factor 2; **E**) were determined by quantitative real-time polymerase chain reaction. Relative mRNA levels were calculated and expressed as fold change over control (value, 1.0) after normalizing for TBP (TATA box binding protein). Data are presented as mean±SEM of at least 3 to 4 independent experiments. Representative Western blot (**F**) shows an increase of OPN in VDR^{wt} VSMCs treated with CM for 6 days and a decrease in VDR^{ko} VSMCs treated with the same conditions. **G**, Quantitative analysis by densitometry. Data were normalized to GAPDH and presented as mean±SEM of 2 independent experiments. *P* values were determined by post hoc pairwise comparisons after 2-way ANOVA. *P*≤0.001 (**C**), *P*=nonsignificant (**D** and **E**), *P*=0.002 (**G**). Scale bar represents 50 and 100 µm.

VSMCs compared with control cells, whereas the absence of VDR from VSMCs blunted the increase of OPN mRNA expression in VDR^{ko} VSMCs incubated in CM (Figure 5D). Protein levels of OPN were strongly increased in VDR^{wt} VSMCs incubated in CM, whereas this increase was much lower in VDR^{ko} VSMCs (Figure 5F and 5G). As seen in our in vivo study, Runx2 showed a tendency to increase in both VDR^{wt} and VDR^{ko} VSMCs treated with CM, regardless of the levels of calcification (Figure 5E).

Altogether, our results imply that the absence of VDR from VSMCs protects against the development of VC in vitro.

VDR From VSMCs Modulates the Expression of miR-145a In Vivo and In Vitro

Taking into consideration the fact that VDR has an influence to a widespread miRNA expression, as well as the fact that a myriad of miRNAs are present in VSMCs, we wished to evaluate the possible involvement of certain miRNAs in VDR-mediated VC. Using the qPCR analysis, we evaluated the arterial expression of various miRNAs reported to be involved in VC and being regulated by VDR. As seen from Figure 6A, the expression of miR-145a showed a marked reduction in the calcified arteries of Cre+ VDR$^{wt/wt}$ mice affected by CKD, which was successfully recovered in the arteries of Cre+ VDR$^{lox/lox}$ littermates, reaching almost similar levels as in the control group (Figure 6A). miR-155 showed tendency to increase in both CKD groups of mice compared with their corresponding controls (Figure 6A); however, we did not detect significant differences between CKD-affected Cre+ VDR$^{wt/wt}$ and Cre+ VDR$^{lox/lox}$ mice. VC had no effects on the levels of miR-29b, miR-30c, and miR-146 in our experimental model of VC in CKD (Figure 6A).

Consistent with in vivo findings, the expression of miR-145a markedly decreased in VDR^{wt} VSMCs treated with CM in vitro (Figure 6B), while its expression recovered in VDR^{ko} VSMCs treated with the same conditions, reaching almost similar levels as in the control group (Figure 6B).

With the aim to confirm the role of VDR in the regulation of miR-145a expression, human and mouse VDR^{wt} VSMCs were treated with 1,25D. Both mice and human normal VSMCs treated with 1.10 and 100 nM 1,25D during 6 days showed a significant decrease of miR-145a expression (Figure 6C), confirming the direct regulation of miR-145a by VDR.

miR-145a Protects Against VC by Modulating the Expression of OPN in VSMCs

To assess the role of miR-145a in the regulation of VSMC's calcification in our study, we overexpressed this miRNA in VDR^{wt} VSMCs. A marked increase of Ca deposition was observed in VSMCs treated with CM, compared with control cells treated with NM (Figure 7B). However, in transfected VDR^{wt} VSMCs with the forced expression of miR-145a (Figure 7A), the increase of Ca content was significantly decreased after 6 days in CM (Figure 7B). Consistently, we have detected a clear effect of miR-145a on the expression of the target gene OPN, showing a significant decrease in VDRwt VSMCs transfected with miR-145a mimic and treated with CM (Figure 7C). Furthermore, a predicted miR-145a–binding site was detected in 3′UTR of OPN mRNA transcript, through the extended seed region of the miRNA. miRBase[38] and UCSC (University of California Santa Cruz) Genome Browser Home[39] were used for the analysis (Figure S4).

Next, we wished to confirm that the modulation of OPN expression goes directly through miR-145a. In the gain-of-function and loss-of-function experiments, we transfected mouse VDR^{wt} VSMCs with miR-145a mimic or miR-145a inhibitor and subsequently treated them with 10 nM 1,25D in NM, as explained in Materials and Methods. Treatment with 1,25D upregulated OPN; however, the forced expression of miR-145a suppressed the expression levels of OPN induced by the VDR agonist (Figure 7D). Furthermore, when miR-145a was inhibited, OPN raised more than in cells treated only with 1,25D. The results obtained here corroborate the fact that miR-145a levels play a crucial role in OPN regulation, preventing its rise (Figure 7F). Finally, we confirmed that this OPN regulation by miR-145a was independent of 1,25D effect on Runx2. There were no significant differences in Runx2 levels in 1,25D-treated cells after transfection with mir-145a mimic or inhibitor (Figure 7E and 7G).

DISCUSSION

In the present study, we demonstrate the role for VSMC's VDR in the regulation of medial VC during CKD and propose a potential functional implication of miR-145a in this process.

VC is a highly frequent complication of CKD and a pivotal risk factor for cardiovascular events and mortality in humans.[40,41] Being controlled by multiple factors, pathogenesis of VC during CKD is not entirely understood. Here, we show that patients with CKD presented increased expression of VDR in their calcified arteries compared with control non-CKD donors. Furthermore, in our experimental model of VC in CKD, mice subjected to 5/6 nephrectomy showed a marked elevation of VDR in arteries affected by calcification. The role of VDR in regulating VC has been previously studied, but conflictive results have been published.[19,20,42] Of note, Han et al[20] demonstrated that VDR^{ko} mice showed reduced VC compared with VDR^{wt} mice in a mouse model of VC induced by high dose of vitamin D. However, Lomashvili et al showed that, in a model of CKD, high doses of vitamin D similarly promoted calcification in transplanted aortic segments from VDR^{ko} into WT animals or vice

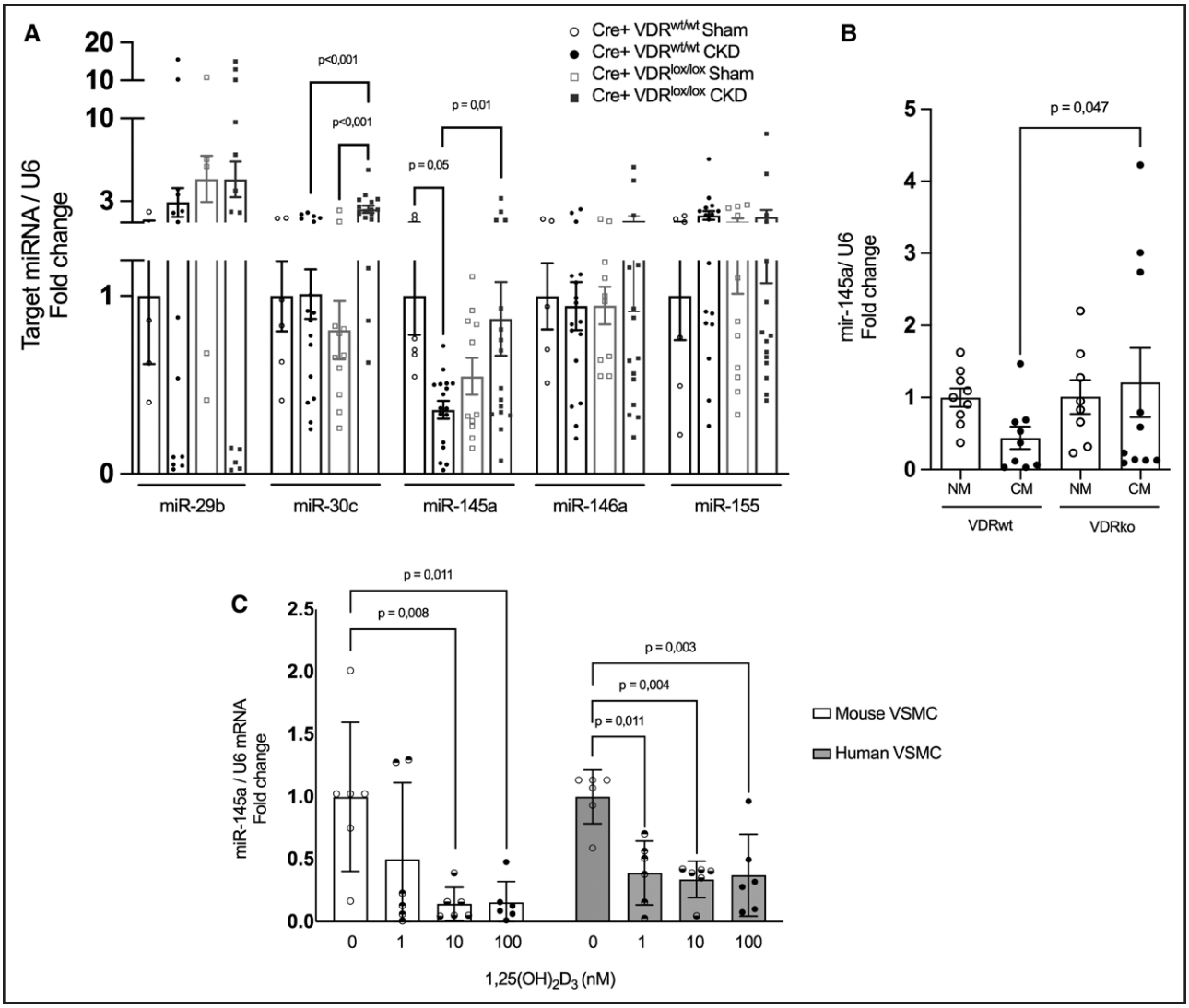

Figure 6. VDR (vitamin D receptor) regulates arterial and vascular smooth muscle cell (VSMC) miR-145a levels during vascular calcification in vivo and in vitro.

Eight-week-old Cre+ VDR$^{wt/wt}$ and Cre+ VDR$^{lox/lox}$ male mice were subjected to subtotal nephrectomy and subsequently treated with high-phosphate diet (HPD) and 1α-25-dihydroxyvitamin D_3 (1,25D) for 2 months to induce vascular calcification (VC), as explained in Materials and Methods. **A**, Total mRNA was extracted from arteries, and levels of miR-29b, miR-30c, miR-145a, miR-146a, and miR-155 were determined by quantitative real-time polymerase chain reaction (PCR). Relative microRNA (miRNA) levels were calculated and expressed as fold change over Sham controls (value, 1.0) after normalizing for U6. Data are presented as mean±SEM (n=4–11 [Sham] or 13–17 [chronic kidney disease (CKD)] mice per group). *P* values were determined by Welch test. **B**, VSMCs were isolated from arteries of VDR^{wt} and VDR^{ko} mice and subsequently incubated in calcification medium (CM) or normal medium (NM) for 6 days, as explained in Materials and Methods. Total mRNA was extracted from VSMCs, and levels of miR-145a were determined by quantitative real-time PCR. **C**, miR-145a expression in mouse and human VDR^{wt} VSMCs treated with increasing 1,25D concentrations (1, 10, and 100 nM) in normal medium with 5% fetal bovine serum (FBS) during 6 days and after. Relative miRNA levels were calculated and expressed as fold change over controls (value, 1.0) after normalizing for U6. Data are presented as mean±SEM of at least 3 to 4 independent experiments. *P* values were determined by post hoc pairwise comparisons after 2-way ANOVA (**A** and **B**) and Kruskal-wallis test (**C**). Mir29b, Mir146a, and Mi1155: *P*=nonsignificant (n.s.); Mir30c: *P*=0.005; Mir145a: *P*=0.007 (**A**); *P*=n.s. (**B**).

versa. Thus, while the presence of physiologically active VDRs in VSMCs is well described, details on its role in regulating medial calcification in CKD are still lacking.

To directly assess the potential role of VSMC's VDR in VC during CKD, we used conditional gene targeting and selectively deleted VDR in mouse arterial VSMCs. We found that Cre+ VDR$^{lox/lox}$ mice affected by CKD showed an evident inhibition of VC compared with Cre+ VDR$^{wt/wt}$ littermates that underwent the same conditions. Thus, levels of Ca deposition in the artery were markedly alleviated in CKD-affected Cre+ VDR$^{lox/lox}$ mice even though both Cre+ VDR$^{wt/wt}$ and Cre+ VDR$^{lox/lox}$ mice had a comparable degree of renal impairment alongside similar levels of serum P and Ca. The protective effect of

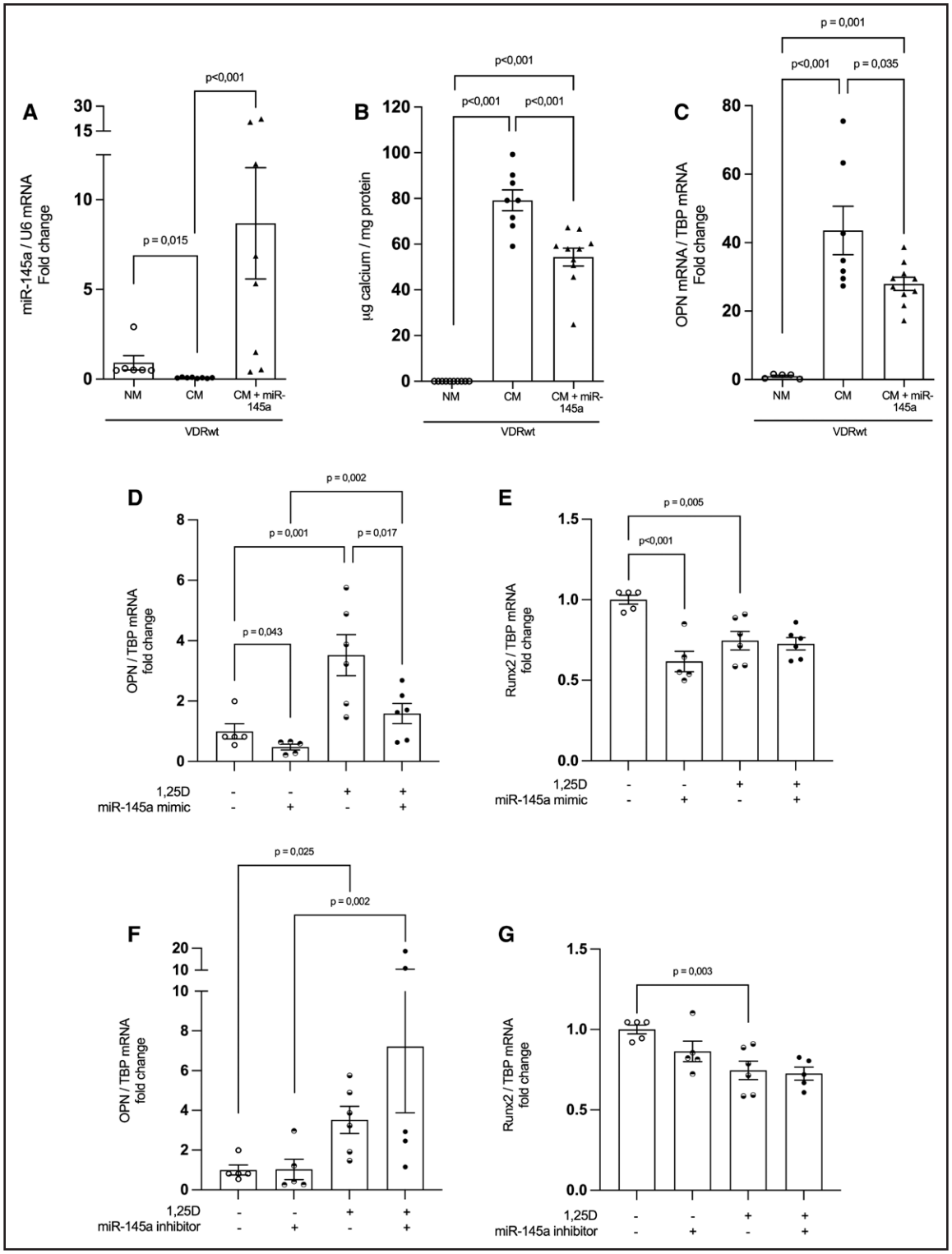

Figure 7. miR-145a inhibits vascular calcification and blunts vitamin d-induced osteopontin increases.
A through **C**, VDR^{wt} vascular smooth muscle cells (VSMCs) were transfected, with mmu-miR-145a-5p mimic or the corresponding scrambled control and subsequently treated with calcification medium (CM), as explained in Materials and Methods. **B**, Quantification of cellular calcium content using the o-cresolphtalein complexone method. Total mRNA was extracted from VSMCs, and mRNAs for miR-145a (**A**) and OPN (osteopontin; **C**) were determined by quantitative real-time polymerase chain reaction (PCR) and normalized to U6 or TBP (TATA box binding protein), respectively. Data are presented as mean±SEM of at least 3 to 4 independent experiments. VDR^{wt} VSMCs treated during 6 days with 10 nM 1α-25-dihydroxyvitamin D_3 (1,25D) together with mmu-miR-145a-5p mimic or mmu-miR-145a-5p inhibitor in normal medium. mRNA levels of OPN (**D** and **F**) and Runx2 (runt-related transcription factor 2; **E** and **G**) were determined by quantitative real-time PCR and normalized to TBP. Data are presented as mean±SEM of 3 independent experiments. *P* values were determined by the Kruskal-Wallis test (**A**–**C**) and post hoc pairwise comparisons after 2-way ANOVA (**D**–**G**). *P*=nonsignificant (**D**, **F**, and **G**), *P*=0.002 (**E**). NM indicates normal medium; VC, vascular calcification; and VDR, vitamin D receptor.

VSMC's VDR deletion against VC seems to engage the modulation of promoters and inhibitors of the calcification process. Indeed, we observed a significant decrease of OPN and lamin A, as well as an increase of SOST in the arteries of CKD-affected Cre+ $VDR^{lox/lox}$ mice, compared with Cre+ $VDR^{wt/wt}$ littermates. The increase of OPN has already been reported in arteries of CKD mice fed a high-phosphate diet and treated with VDR agonists.[43] Indeed, OPN has a vitamin D response element; therefore, VDR can have a direct effect on OPN expression,[13] and some reports have suggested that OPN is an inductor of VC.[13,44,45] Lau et al[43] detected an increase of secreted OPN in VSMCs after treatment with an active vitamin D compound, suggesting that the increase of OPN was mediated by VDR agonist. Results of our study show that the deletion of VDR from VSMCs led to a significant alleviation of VC accompanied with the marked decrease of OPN in mouse arteries. Another protein involved in VC, lamin A, showed a marked upregulation in calcified arteries of Cre+ $VDR^{wt/wt}$ mice, which was successfully alleviated in arteries of Cre+ $VDR^{lox/lox}$ counterparts. Quirós-González et al[9] demonstrated an increase of lamin A during calcification of VMSCs in vitro and in vivo, whereas Almofti et al[10] detected an upregulation of lamin A in rat aortas treated with vitamin D. Finally, SOST, described as a VC inhibitor, markedly decreased in calcified arteries of Cre+ $VDR^{wt/wt}$ mice affected by CKD in our study, while its expression recovered in arteries of Cre+ $VDR^{lox/lox}$ littermates. Indeed, several studies demonstrated the protective role of SOST against VC,[11,12,46] showing its capacity to diminish Ca deposition in vitro,[46] modulate VSMC transdifferentiation to osteoblastic cells, as well as to regulate the expression of OPN in mouse arteries.[11] Interestingly, Runx2—a major pro-osteoblastic transcription factor—was increased in arteries of both Cre+ $VDR^{wt/wt}$ and Cre+ $VDR^{lox/lox}$ mice affected by CKD, independently of the level of calcification. This result indicates that Runx2 is necessary, but not sufficient, to promote VC in vivo.

Our results are in disagreement with those of Lomashvili et al,[19] in which transplantation of arteries from VDR^{wt} animals into VDR^{ko} and vice versa did not show differences in calcification. However, in those experiments, all the cellular types in the transplanted segment (namely, endothelial, smooth muscle, and pericyte cells) preserved the original genotype, which could lead to different results. In our case, the specific role of VSMC VDR is assessed, clearly showing that lack of vitamin D signaling in this cell type leads to lower VC. There is also an apparent discrepancy between our results and those of Carrillo-Lopez et al.[47] In their study, the authors showed that treatment of CKD mice with vitamin D induced an increase in miR-145 in the arteries. However, in their study, they administered the synthetic VDRA (vitamin D receptor agonist) paricalcitol (19-nor $1,25[OH]_2D_2$), whereas we use the animal form of active vitamin D (1,25D). Indeed, we and others have shown that both compounds have a significant difference in VC, being paricalcitol significantly less procalcificant than 1,25D.[42,48] Thus, we believe that the results are not contradictory but might even partly explain the differences in calcification exerted by both compounds.

The effect of impaired VDR signaling on VSMC's calcification was corroborated in our in vitro study using primary mouse VSMCs from VDR^{wt} and VDR^{ko} mice. Thus, the absence of VDR prevented calcification of VSMCs, which was accompanied by a marked decrease of OPN. Runx2 showed tendency to increase in both VDR^{wt} and VDR^{ko} VSMCs treated with CM, but without significant differences, as seen in our in vivo study. Of note, Han et al[20] demonstrated the existence of the functional cooperation between VDR and Runx2 in osteoblastic differentiation of VSMCs, in addition to their described physical interaction. The fact that Runx2 can interact with VSMC's VDR and thus promote calcification could partially explain why the arteries of our Cre+ $VDR^{lox/lox}$ mice in vivo, as well as VDR^{ko} VSMCs in vitro do not present high Ca deposition, even though they have increased expression of Runx2. Additionally, the potential of Runx2 to regulate OPN transcription, which can be increased with the synergic interaction between Runx2 and VDR,[49] indicates that the observed differences in calcification in our in vitro and in vivo studies could be mediated by OPN.

VDR has been proposed to regulate a widespread miRNA expression in different cells and tissues. Furthermore, miRNAs have been described to be present in VSMCs and actively involved in the VC process.[22,23] In our study, we assessed the expression of certain miRNAs associated with VC and known to be regulated by VDR. miR-145a showed to be significantly decreased in calcified arteries of Cre+ $VDR^{wt/wt}$ mice affected by CKD, while VDR deletion from VSMCs restored its expression in Cre+ $VDR^{lox/lox}$ littermates. The results were corroborated in our in vitro study where lower expression of miR-145a was detected in VSMCs treated with CM, as well as in mice with VC.[26] In those mice, miR-155 showed a tendency to increase in both groups of CKD mice, while the levels of miR-29b, miR-30c, and miR-146 did not substantially change. It has been reported that VDR could regulate miR-145a[27] and that this miRNA has an important role in the phenotypic change of VSMCs.[50,51] We confirmed this direct effect of VDR signaling on miR-145a expression through our in vitro experiments with both human and mice VSMCs, in which incubation with 1,25D induced a reduction of the miR-145a levels. To assess the role of miR-145a in the regulation of VSMC's calcification in our in vitro study, we overexpressed this miRNA in VDR^{wt} VSMCs. Forced expression of miR-145a in VSMCs in vitro led to a significant reduction of Ca deposition alongside lower OPN expression, pointing to OPN as a possible target of mir-145a during VC in CKD.

Importantly, gain-of-function and loss-of-function experiments confirmed that the modulation of OPN expression goes directly through miR-145a. On one side, 1,25D treatment upregulated OPN, and the forced expression of miR-145a suppressed the levels of OPN induced by this agonist. On the other side, the inhibition of miR-145a led to a significant increase in OPN levels, even higher than in cells treated solely with 1,25D. The results obtained here corroborate the fact that miR-145a levels play a crucial role in OPN regulation, preventing its increase.

We conclude that VDR is induced in calcified VSMCs during CKD where it can modulate the expression of promoters and inhibitors of VSMC transdifferentiation, as well as small noncoding RNA molecules such as miR-145a that contribute to VC. The regulation of these pathways by VDR seems to be essential for the settings of CKD-induced VC as deletion of VDR from VSMCs prevented it. Development of a possible therapeutic approach to inhibit VSMC's VDR to prevent VC during CKD warrants further investigation.

ARTICLE INFORMATION

Received November 24, 2022; accepted June 13, 2023.

Affiliations

Vascular and Renal Translational Research Group, Institute for Biomedical Research in Lleida, Spain (M.C., M.M.-A., M.B., J.M.V.). Bone and Mineral Research Unit, Hospital Universitario Central de Asturias, Instituto de Investigación Sanitaria del Principado de Asturias, Oviedo, Spain (C.A.-M., J.L.F.-M.). Redes de Investigación Cooperativa Orientadas a Resultados en Salud, RICORS2040 (Kidney Disease), Madrid, Spain (C.A.-M., J.L.F.-M.).

Acknowledgments

The authors thank Alicia Garcia, Ana Martinez, Aurora Pérez, and Àuria Eritja for their technical help in the laboratory.

Sources of Funding

This research was supported by research grants PI18/00292, PI18/00610, PI21/00204, and PI21/01099 from Instituto de Salud Carlos III (ISCIII) and FEDER funds Una manera de hacer Europa. M. Caus was supported by studentship from the Agència de Gestió d'Ajuts Universitaris i de Recerca of the Catalan Government (AGAUR), Diputació de Lleida, and Red de Investigacion Renal (RETIC RedInRen). M. Bozic was supported by the Miguel Servet contract from ISCIII (CP19/00027) financed by Fondo Social Europeo El FSE invierte en tu futuro.

Disclosures

None.

Supplemental Material

Expanded Materials & Methods
Figures S1–S4
Table S1
Major Resources Table
Animal Research: Reporting of In Vivo Experiments (ARRIVE) Guidelines
Full Unedited Blots

REFERENCES

1. Vervloet M, Cozzolino M. Vascular calcification in chronic kidney disease: different bricks in the wall? *Kidney Int*. 2017;91:808–817. doi: 10.1016/j.kint.2016.09.024
2. Liu ZH, Yu XQ, Yang JW, Jiang AL, Liu BC, Xing CY, Lou JZ, Wang M, Cheng H, Liu J, et al; China Dialysis Calcification Study Group. Prevalence and risk factors for vascular calcification in Chinese patients receiving dialysis: baseline results from a prospective cohort study. *Curr Med Res Opin*. 2018;34:1491–1500. doi: 10.1080/03007995.2018.1467886
3. Okuno S, Ishimura E, Kitatani K, Fujino Y, Kohno K, Maeno Y, Maekawa K, Yamakawa T, Imanishi Y, Inaba M, et al. Presence of abdominal aortic calcification is significantly associated with all-cause and cardiovascular mortality in maintenance hemodialysis patients. *Am J Kidney Dis*. 2007;49:417–425. doi: 10.1053/j.ajkd.2006.12.017
4. Bozic M, Méndez-Barbero N, Gutiérrez-Muñoz C, Betriu A, Egido J, Fernández E, Martín-Ventura JL, Valdivielso JM, Blanco-Colio LM; Investigators From the NEFRONA Study. Combination of biomarkers of vascular calcification and sTWEAK to predict cardiovascular events in chronic kidney disease. *Atherosclerosis*. 2018;270:13–20. doi: 10.1016/j.atherosclerosis.2018.01.011
5. Waziri B, Duarte R, Naicker S. Chronic kidney disease – mineral and bone disorder (CKD-MBD): current perspectives. *Int J Nephrol Renovasc Dis*. 2019;12:263–276. doi: 10.2147/IJNRD.S191156
6. Durham AL, Speer MY, Scatena M, Giachelli CM, Shanahan CM. Role of smooth muscle cells in vascular calcification: implications in atherosclerosis and arterial stiffness. *Cardiovasc Res*. 2018;114:590–600. doi: 10.1093/cvr/cvy010
7. Paloian NJ, Giachelli CM. A current understanding of vascular calcification in CKD. *Am J Physiol Ren Physiol*. 2014;307:F891–F900. doi: 10.1152/ajprenal.00163.2014
8. Karwowski W, Naumnik B, Szczepański M, Myśliwiec M. The mechanism of vascular calcification - a systematic review. *Med Sci Monit*. 2012;18:RA1–R11. doi: 10.12659/msm.882181
9. Quirós-González I, Román-García P, Alonso-Montes C, Barrio-Vázquez S, Carrillo-López N, Naves-Díaz M, Mora MI, Corrales FJ, López-Hernández FJ, Ruiz-Torres MP, et al. Lamin A is involved in the development of vascular calcification induced by chronic kidney failure and phosphorus load. *Bone*. 2016;84:160–168. doi: 10.1016/j.bone.2016.01.005
10. Almofti MR, Huang Z, Yang P, Rui Y, Yang P. Proteomic analysis of rat aorta during atherosclerosis induced by high cholesterol diet and injection of vitamin D3. *Clin Exp Pharmacol Physiol*. 2006;33:305–309. doi: 10.1111/j.1440-1681.2006.04366.x
11. Krishna SM, Seto SW, Jose RJ, Li J, Morton SK, Biros E, Wang Y, Nsengiyumva V, Lindeman JHN, Loots GG, et al. Wnt signaling pathway inhibitor sclerostin inhibits angiotensin II-induced aortic aneurysm and atherosclerosis. *Arterioscler Thromb Vasc Biol*. 2017;37:553–566. doi: 10.1161/ATVBAHA.116.308723
12. Nguyen-Yamamoto L, Tanaka KI, St-Arnaud R, Goltzman D. Vitamin D-regulated osteocytic sclerostin and BMP2 modulate uremic extraskeletal calcification. *JCI insight*. 2019;4:e126467. doi: 10.1172/jci.insight.126467
13. Jono S, Nishizawa Y, Shioi A, Morii H. 1,25-dihydroxyvitamin D3 increases in vitro vascular calcification by modulating secretion of endogenous parathyroid hormone-related peptide. *Circulation*. 1998;98:1302–1306. doi: 10.1161/01.cir.98.13.1302
14. Noda M, Vogel RL, Craig AM, Prahl J, DeLuca HF, Denhardt DT. Identification of a DNA sequence responsible for binding of the 1,25-dihydroxyvitamin D3 receptor and 1,25-dihydroxyvitamin D3 enhancement of mouse secreted phosphoprotein 1 (Spp-1 or osteopontin) gene expression. *Proc Natl Acad Sci USA*. 1990;87:9995–9999. doi: 10.1073/pnas.87.24.9995
15. Kawashima H. Receptor for 1,25-dihydroxyvitamin D in a vascular smooth muscle cell line derived from rat aorta. *Biochem Biophys Res Commun*. 1987;146:1–6. doi: 10.1016/0006-291x(87)90681-4
16. Drüeke TB, Massy ZA. Role of vitamin D in vascular calcification: bad guy or good guy? *Nephrol Dial Transplant*. 2012;27:1704–1707. doi: 10.1093/ndt/gfs046
17. Shroff R, Egerton M, Bridel M, Shah V, Donald AE, Cole TJ, Hiorns MP, Deanfield JE, Rees L. A bimodal association of vitamin D levels and vascular disease in children on dialysis. *J Am Soc Nephrol*. 2008;19:1239–1246. doi: 10.1681/ASN.2007090993
18. Wang J, Zhou JJ, Robertson GR, Lee VW. Vitamin D in vascular calcification: a double-edged sword? *Nutrients*. 2018;10:652. doi: 10.3390/nu10050652
19. Lomashvili KA, Wang X, O'Neill WC. Role of local versus systemic vitamin D receptors in vascular calcification. *Arterioscler Thromb Vasc Biol*. 2014;34:146–151. doi: 10.1161/ATVBAHA.113.302525
20. Han MS, Che X, Cho G, Park HR, Lim KE, Park NR, Jin JS, Jung YK, Jeong JH, Lee IK, et al. Functional cooperation between vitamin D receptor and Runx2 in vitamin D-induced vascular calcification. *PLoS One*. 2013;8:e83584. doi: 10.1371/journal.pone.0083584
21. Valdivielso JM, Coll B, Fernandez E. Vitamin D and the vasculature: can we teach an old drug new tricks? *Expert Opin Ther Targets*. 2009;13:29–38. doi: 10.1517/14728220802564390

22. Leopold JA. MicroRNAs regulate vascular medial calcification. *Cells*. 2014;3:963–980. doi: 10.3390/cells3040963
23. Kim YK, Kook H. Diverse roles of noncoding RNAs in vascular calcification. *Arch Pharm Res*. 2019;42:244–251. doi: 10.1007/s12272-019-01118-z
24. Caus M, Eritja A, Bozic M. Role of microRNAs in obesity-related kidney disease. *Int J Mol Sci*. 2021;22:11416. doi: 10.3390/ijms222111416
25. Chen NX, Kiattisunthorn K, O'Neill KD, Chen X, Moorthi RN, Gattone VH, Allen MR, Moe SM. Decreased microRNA is involved in the vascular remodeling abnormalities in chronic kidney disease (CKD). *PLoS One*. 2013;8:e64558. doi: 10.1371/journal.pone.0064558
26. Rangrez AY, M'Baya-Moutoula E, Metzinger-Le Meuth V, Hénaut L, Djelouat MSI, Benchitrit J, Massy ZA, Metzinger L. Inorganic phosphate accelerates the migration of vascular smooth muscle cells: evidence for the involvement of miR-223. *PLoS One*. 2012;7:e47807. doi: 10.1371/journal.pone.0047807
27. Chang S, Gao L, Yang Y, Tong D, Guo B, Liu L, Li Z, Song T, Huang C. miR-145 mediates the antiproliferative and gene regulatory effects of vitamin D3 by directly targeting E2F3 in gastric cancer cells. *Oncotarget*. 2015;6:7675–7685. doi: 10.18632/oncotarget.3048
28. Kallay E, Pietschmann P, Toyokuni S, Bajna E, Hahn P, Mazzucco K, Bieglmayer C, Kato S, Cross HS. Characterization of a vitamin D receptor knockout mouse as a model of colorectal hyperproliferation and DNA damage. *Carcinogenesis*. 2001;22:1429–1435. doi: 10.1093/carcin/22.9.1429
29. Van Cromphaut SJ, Dewerchin M, Hoenderop JGJ, Stockmans I, Van Herck E, Kato S, Bindels RJ, Collen D, Carmeliet P, Bouillon R, et al. Duodenal calcium absorption in vitamin D receptor-knockout mice: functional and molecular aspects. *Proc Natl Acad Sci USA*. 2001;98:13324–13329. doi: 10.1073/pnas.231474698
30. Marchesi C, Rehman A, Rautureau Y, Kasal DA, Briet M, Leibowitz A, Simeone SMC, Ebrahimian T, Neves MF, Offermanns S, et al. Protective role of vascular smooth muscle cell PPARγ in angiotensin II-induced vascular disease. *Cardiovasc Res*. 2013;97:562–570. doi: 10.1093/cvr/cvs362
31. Torremadé N, Bozic M, Goltzman D, Fernandez E, Valdivielso JM. Effects of the administration of 25(OH) vitamin D3 in an experimental model of chronic kidney disease in animals null for 1-alpha-hydroxylase. *PLoS One*. 2017;12:e0170654–e0170614. doi: 10.1371/journal.pone.0170654
32. Bozic M, de Rooij J, Parisi E, Ortega MR, Fernandez E, Valdivielso JM. Glutamatergic signaling maintains the epithelial phenotype of proximal tubular cells. *J Am Soc Nephrol*. 2011;22:1099–1111. doi: 10.1681/ASN.2010070701
33. Bozic M, Caus M, Rodrigues-Diez RR, Pedraza N, Ruiz-Ortega M, Garí E, Gallel P, Panadés MJ, Martinez A, Fernández E, et al. Protective role of renal proximal tubular alpha-synuclein in the pathogenesis of kidney fibrosis. *Nat Commun*. 2020;11:1943. doi: 10.1038/s41467-020-15732-9
34. Arcidiacono MV, Carrillo-López N, Panizo S, Castro-Grattoni AL, Valcheva P, Ulloa C, Rodríguez-Carrio J, Cardús A, Quirós-Caso C, Martínez-Arias L, et al. Barley-ß-glucans reduce systemic inflammation, renal injury and aortic calcification through ADAM17 and neutral-sphingomyelinase2 inhibition. *Sci Rep*. 2019;9:17810. doi: 10.1038/s41598-019-54306-8
35. Valcheva P, Cardus A, Panizo S, Parisi E, Bozic M, Lopez Novoa JM, Dusso A, Fernández E, Valdivielso JM. Lack of vitamin D receptor causes stress-induced premature senescence in vascular smooth muscle cells through enhanced local angiotensin-II signals. *Atherosclerosis*. 2014;235:247–255. doi: 10.1016/j.atherosclerosis.2014.05.911
36. Pickering JG, Weir L, Rosenfield K, Stetz J, Jekanowski J, Isner JM. Smooth muscle cell outgrowth from human atherosclerotic plaque: implications for the assessment of lesion biology. *J Am Coll Cardiol*. 1992;20:1430–1439. doi: 10.1016/0735-1097(92)90259-p
37. Torremadé N, Bozic M, Panizo S, Barrio-Vazquez S, Fernandez-Martín JL, Encinas M, Goltzman D, Arcidiacono MV, Fernandez E, Valdivielso JM. Vascular calcification induced by chronic kidney disease is mediated by an increase of 1α-hydroxylase expression in vascular smooth muscle cells. *J Bone Miner Res*. 2016;31:1865–1876. doi: 10.1002/jbmr.2852
38. Griffiths-Jones S. The microRNA registry. *Nucleic Acids Res*. 2004;32:D109–D111. doi: 10.1093/nar/gkh023
39. Kent WJ, Sugnet CW, Furey TS, Roskin KM, Pringle TH, Zahler AM, Haussler D. The human genome browser at UCSC. *Genome Res*. 2002;12:996–1006. doi: 10.1101/gr.229102
40. Sigrist M, Bungay P, Taal MW, McIntyre CW. Vascular calcification and cardiovascular function in chronic kidney disease. *Nephrol Dial Transplant*. 2006;21:707–714. doi: 10.1093/ndt/gfi236
41. Rennenberg RJMW, Kessels AGH, Schurgers LJ, Van Engelshoven JMA, De Leeuw PW, Kroon AA. Vascular calcifications as a marker of increased cardiovascular risk: a meta-analysis. *Vasc Health Risk Manag*. 2009;5:185–197. doi: 10.2147/vhrm.s4822
42. Cardús A, Panizo S, Parisi E, Fernandez E, Valdivielso JM. Differential effects of vitamin D analogs on vascular calcification. *J Bone Miner Res*. 2007;22:860–866. doi: 10.1359/jbmr.070305
43. Lau WL, Leaf EM, Hu MC, Takeno MM, Kuro-o M, Moe OW, Giachelli CM. Vitamin D receptor agonists increase klotho and osteopontin while decreasing aortic calcification in mice with chronic kidney disease fed a high phosphate diet. *Kidney Int*. 2012;82:1261–1270. doi: 10.1038/ki.2012.322
44. Shioi A, Nishizawa Y, Jono S, Koyama H, Hosoi M, Morii H. β-Glycerophosphate accelerates calcification in cultured bovine vascular smooth muscle cells. *Arterioscler Thromb Vasc Biol*. 1995;15:2003–2009. doi: 10.1161/01.atv.15.11.2003
45. Grand Moursel L, van der Graaf LM, Bulk M, van Roon-Mom WMC, van der Weerd L. Osteopontin and phospho-SMAD2/3 are associated with calcification of vessels in D-CAA, an hereditary cerebral amyloid angiopathy. *Brain Pathol*. 2019;29:793–802. doi: 10.1111/bpa.12721
46. McArthur KM, Kay AM, Mosier JA, Grant JN, Stewart JA, Simpson CL. Manipulating the plasticity of smooth muscle cells to regulate vascular calcification. *AIMS Cell Tissue Eng*. 2017;1:165–179.
47. Carrillo-lópez N, Panizo S, Arcidiacono MV, de la Fuente S, Martínez-Arias L, Ottaviano E, Ulloa C, Ruiz-Torres MP, Rodríguez I, Cannata-Andía JB, et al. Vitamin D treatment prevents uremia-induced reductions in aortic microRNA-145 attenuating osteogenic differentiation despite hyperphosphatemia. *Nutrients*. 2022;14:2589. doi: 10.3390/nu14132589
48. Mizobuchi M, Finch JL, Martin DR, Slatopolsky E. Differential effects of vitamin D receptor activators on vascular calcification in uremic rats. *Kidney Int*. 2007;72:709–715. doi: 10.1038/sj.ki.5002406
49. Sowa AK, Kaiser FJ, Eckhold J, Kessler T, Aherrahrou R, Wrobel S, Kaczmarek PM, Doehring L, Schunkert H, Erdmann J, et al. Functional interaction of osteogenic transcription factors Runx2 and VDR in transcriptional regulation of Opn during soft tissue calcification. *Am J Pathol*. 2013;183:60–68. doi: 10.1016/j.ajpath.2013.03.007
50. Rangrez AY, Massy ZA, Metzinger-Le Meuth V, Metzinger L. miR-143 and miR-145: molecular keys to switch the phenotype of vascular smooth muscle cells. *Circ Cardiovasc Genet*. 2011;4:197–205. doi: 10.1161/CIRCGENETICS.110.958702
51. Cheng Y, Liu X, Yang J, Lin Y, Xu DZ, Lu Q, Deitch EA, Huo Y, Delphin ES, Zhang C. MicroRNA-145, a novel smooth muscle cell phenotypic marker and modulator, controls vascular neointimal lesion formation. *Circ Res*. 2009;105:158–166. doi: 10.1161/CIRCRESAHA.109.197517